Electronic Supplementary Material (ESI) for Physical Chemistry Chemical Physics.


Electronic Supplementary Information

# Photoswitchable de/adsorption of azobenzene-derived surfactant on silica surface

Ziye Wu[ab⊥], Xin Li[b⊥], Xiaoming Jiang[c⊥], Tian Xie[d], Huiyong Li[d], Guozhen Zhang*[b], Jun Jiang[b]

[a]School of Information, Guizhou University of Finance and Economics, Guiyang 550025, China

[b]Hefei National Laboratory for Physical Sciences at the Microscale, CAS Center for Excellence in Nanoscience, School of Chemistry and Materials Science, University of Science and Technology of China, Hefei, Anhui 230026, China

[c]Department of chemistry and chemical engineering, Guizhou University, Guiyang 550025, China

[d]State Key Laboratory of Efficient Utilization for Low Grade Phosphate Rock and Its Associated Resources, Wengfu Group, Guiyang 550014, China

*Corresponding author e-mail: guozhen@ustc.edu.cn

## S1. Computational methods

Equilibrium structures of AzoTMA and the tail molecules were optimized by the density functional theory (DFT) methods with the CAM-B3LYP[1] functional at 6-311++G(d,p) level in Gaussian 09 program.[2] Polarizable continuum model (PCM)[3] was used to account for the solvent effect and the solvent is water. Merz-Kollman (MK)[4] method was used to compute the electrostatic potential (ESP) atomic charge. Time-dependent density functional theory (TDDFT)[5] calculations at the same theoretical level were performed to simulate the electronic excited states. Solvation free energy was calculated by the PCM-UAHF[6] method at the level of theory that it was parametrized (HF/6-31G*).[7] Nuclear magnetic resonance (NMR) simulations were performed at B3LYP/TZVP level.

In order to precisely describe the interaction between solute and solvent molecules, we carried out UFF (universal force field) → semi-empirical → DFT three-stage simulation. We first used Packmol[8] package to build the initial configuration in which the solute molecule was surrounded by solvent sphere (radius of the sphere was set to 13 Å and the number of water molecules was 650). The obtained configuration was simply optimized under the molecular mechanics force field UFF in Gaussian 09. Then the solute molecule and the solvent layer were intercepted (the solvent layer thickness was set to 3, 4, 5 Å, corresponding number of water molecules was 50, 68, 110, respectively). The solute-solvent cluster models were pre-optimized by the semiempirical method PM6-D3H4[9,10] in MOPAC (Molecular Orbital PACkage)[11]. Accurate configuration optimizations were performed at the DFT level B3LYP/6-

31+G(d,p) in Gaussian 09, in which dispersion-corrected density functional theory (DFT-D3)[12] calculations were used for the intermolecular interactions. Solute-solvent interaction energy of each configuration was calculated at the same DFT level, and defined as $E_{int} = E_{com\_solute} + E_{com\_water} - E_{com}$, where $E_{com}$ is the energy of the whole complex system consisting of solute and solvent molecules, $E_{com\_solute}$ and $E_{com\_water}$ are the individual energies of the part of solute and the part of solvent molecules with their geometries in the complex system, respectively. $E_{int}$ describes only the interaction between solute and solvent molecules, regardless of the molecular deformation and the interaction between solvent molecules.

Optimizations of the adsorption geometries of AzoTMA on α-quartz(001) surface were performed by the Vienna Ab-initio Simulation Package (VASP) at the DFT level,[13] in which a plane wave basis sets were used to solve the Kohn–Sham equations. The generalized gradient approximation (GGA) with the Perdew–Burke–Ernzerhof (PBE) functional were employed.[14] The periodic boundary condition (PBC) was applied and a 30 Å vacuum layer was used to avoid possible interactions. The energy cutoff for the pane wave expansion was 500eV. Van der Waals (vdW) interaction between the substrate and the adsorbed molecule was described by the density functional dispersion correction method DFT-D2.[15] A 4×4 unit cell of hydroxylated α-quartz(001) surface was chosen as supercell to avoid the intermolecular interactions of AzoTMA. The adsorption energy is calculated by $E_{ads} = E_{sub} + E_{ad} - E_{com}$, where the $E_{com}$, $E_{sub}$ and $E_{ad}$ are energies of the complex, the adsorbent and the adsorbate molecule, respectively. In the case of the intermolecular interaction calculation, we

simulated the adsorption of *trans/cis*-AzoTMA molecule on hydroxylated α-quartz(001) surface in a 1×1/2×1 unit cell and the intermolecular interaction energy is defined as $E_{\text{int}}^{tran/cis} = E_{\text{com\_4×4}} - E_{\text{com\_n×1}} - \Delta E_{\text{surf}}$ (n is 1 for *trans* and 2 for *cis*), where the $E_{\text{com\_4×4}}$ ($E_{\text{com\_n×1}}$) is the energy of the complex system with adsorbed nanostructure in a 4×4 (n×1) supercell, and $\Delta E_{\text{surf}}$ is the energy difference between the 4×4 and n×1 supercell of α-quartz(001) surface.

**S2. NMR and charge distributions**

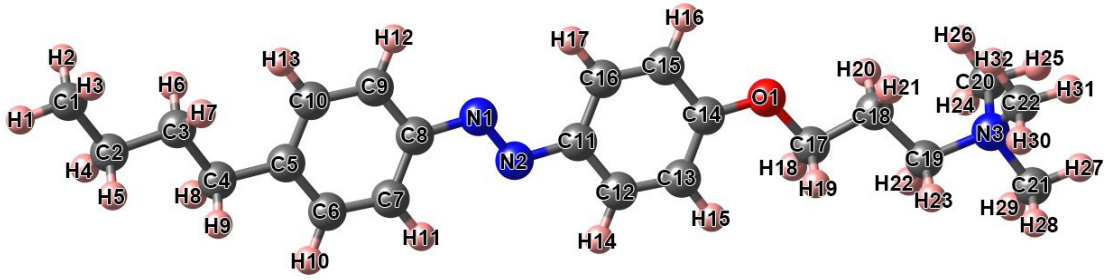


**Fig. S1.** Atomic symbols and labels of AzoTMA molecule.

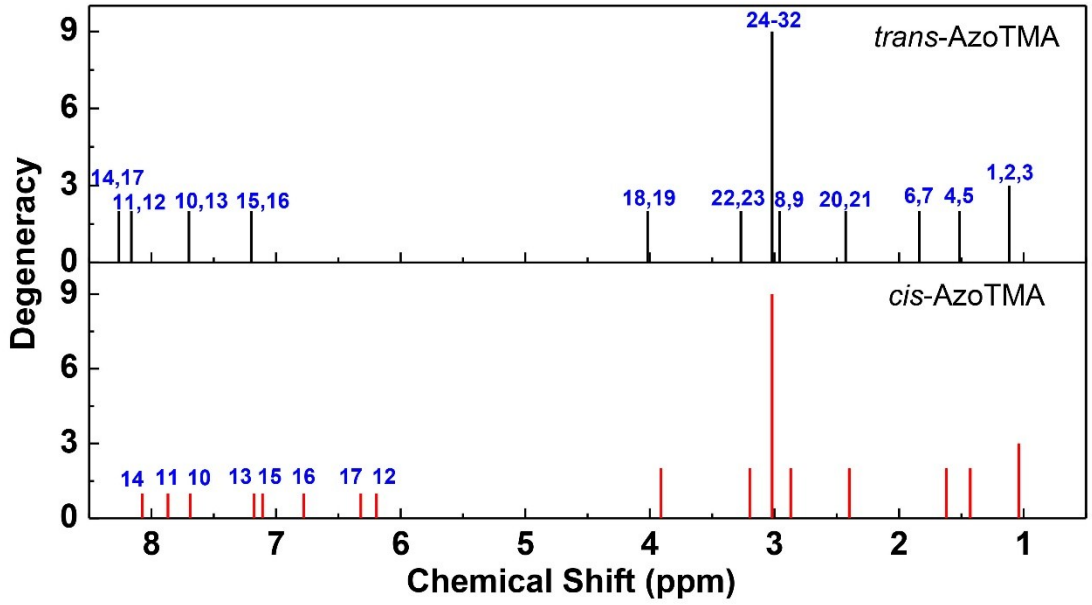


**Fig. S2.** Computed $^{1}$H NMR spectra of *trans*- and *cis*-AzoTMA. Blue number is the label of hydrogen atom corresponding to the NMR signal. The detailed data of chemical shift is shown in Table S1.

As shown in Fig. S2, the NMR spectra of *trsns*- and *cis*-AzoTMA differ markedly in the region of aromatic protons (H10-17). The other regions change a little with the variation of molecular structure. According to Fig. S2, the measured signals in $^{1}$H NMR spectrum of AzoTMA (Fig. 2c) can be contributed to:

0.56 ppm (3H, $CH_3$), 0.92 ppm (2H, $CH_2$), 1.10 ppm (2H, $CH_2$), 1.73 ppm (2H, $CH_2$),

2.05 ppm (2H, $CH_2$), 2.86 ppm (9H, $CH_3$), 3.14 ppm (2H, $CH_2$), 3.53 ppm (2H, $CH_2$), 6.64 ppm (4H, *Ar-H*), 7.32 ppm (4H, *Ar-H*).

Table S1. Chemical shift of hydrogen atoms in *trans*- and *cis*-AzoTMA calculated at B3LYP/TZVP level (the reference is TMS)

| **Label of hydrogen atom** | **Chemical shift (ppm)** | |
|---|---|---|
| | ***trans*** | ***cis*** |
| 1 | 1.24 | 1.19 |
| 2 | 1.06 | 0.96 |
| 3 | 1.05 | 0.98 |
| 4 | 1.53 | 1.41 |
| 5 | 1.51 | 1.45 |
| 6 | 1.97 | 1.65 |
| 7 | 1.72 | 1.60 |
| 8 | 3.00 | 2.86 |
| 9 | 2.92 | 2.89 |
| 10 | 7.63 | 7.69 |
| 11 | 8.16 | 7.87 |
| 12 | 8.16 | 6.19 |
| 13 | 7.76 | 7.18 |
| 14 | 8.24 | 8.07 |
| 15 | 7.12 | 7.11 |
| 16 | 7.34 | 6.78 |
| 17 | 8.28 | 6.32 |
| 18 | 4.03 | 3.92 |
| 19 | 4.01 | 3.90 |
| 20 | 2.46 | 2.43 |
| 21 | 2.42 | 2.38 |
| 22 | 3.27 | 3.23 |
| 23 | 3.27 | 3.17 |
| 24 | 2.82 | 2.81 |
| 25 | 2.89 | 2.90 |
| 26 | 3.27 | 3.27 |
| 27 | 3.00 | 3.05 |
| 28 | 3.11 | 3.06 |
| 29 | 3.10 | 3.08 |
| 30 | 2.79 | 2.78 |
| 31 | 2.95 | 2.98 |
| 32 | 3.23 | 3.24 |

Table S2. Electrostatic potential (ESP) charges of *trans*- and *cis*-AzoTMA (charges on hydrogens are summed into heavy atoms)

| **Atoms** | **Charge (e)** | |
|---|---|---|
| | ***trans*** | ***cis*** |
| **C1** | -0.105 | -0.108 |
| **C2** | 0.101 | 0.091 |
| **C3** | 0.153 | 0.162 |
| **C4** | -0.174 | -0.126 |
| **C5** | 0.241 | 0.132 |
| **C6** | -0.146 | -0.041 |
| **C7** | 0.004 | -0.207 |
| **C8** | 0.348 | 0.769 |
| **C9** | -0.128 | -0.360 |
| **C10** | -0.040 | 0.080 |
| **N1** | -0.286 | -0.415 |
| **N2** | -0.228 | -0.387 |
| **C11** | 0.248 | 0.727 |
| **C12** | -0.067 | -0.385 |
| **C13** | -0.118 | 0.072 |
| **C14** | 0.503 | 0.424 |
| **C15** | -0.213 | -0.159 |
| **C16** | 0.088 | -0.081 |
| **O1** | -0.528 | -0.516 |
| **C17** | 0.378 | 0.345 |
| **C18** | 0.146 | 0.184 |
| **C19** | -0.028 | -0.035 |
| **N3** | 0.372 | 0.351 |
| **C20** | 0.167 | 0.137 |
| **C21** | 0.141 | 0.176 |
| **C22** | 0.169 | 0.170 |

Table S3. ESP charges of *trans* and *cis* tail (charges on hydrogens are summed into heavy atoms)

| **Atoms** | **Charge (e)** | |
|---|---|---|
| | ***trans*** | ***cis*** |
| **C1** | -0.108 | -0.087 |
| **C2** | 0.110 | 0.069 |
| **C3** | 0.146 | 0.162 |

| | | |
|---|---|---|
| **C4** | -0.169 | -0.127 |
| **C5** | 0.234 | 0.165 |
| **C6** | -0.143 | -0.062 |
| **C7** | 0.001 | -0.164 |
| **C8** | 0.340 | 0.685 |
| **C9** | -0.130 | -0.290 |
| **C10** | -0.031 | 0.039 |
| **N1** | -0.288 | -0.425 |
| **N2** | -0.220 | -0.372 |
| **C11** | 0.220 | 0.584 |
| **C12** | -0.066 | -0.280 |
| **C13** | -0.125 | -0.012 |
| **C14** | 0.545 | 0.516 |
| **C15** | -0.235 | -0.216 |
| **C16** | 0.101 | -0.008 |
| **O1** | -0.556 | -0.562 |
| **C17** | 0.319 | 0.337 |
| **C18** | 0.149 | 0.134 |
| **C19** | -0.096 | -0.087 |

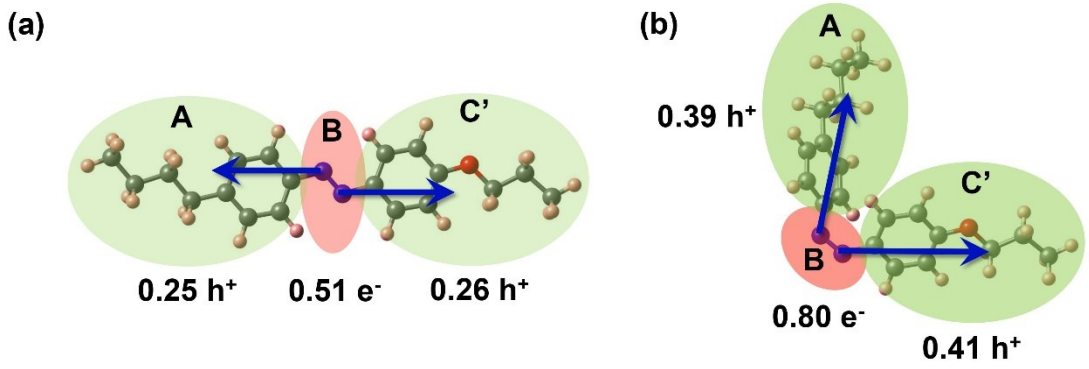


**Fig. S3.** Charge distributions in three parts of the tail molecule in *trans* (a) and *cis* (b) form together with charge polarization directions, obtained by ESP charge analysis. The $h^+$ ($e^-$) represents a positive (negative) elementary charge. The green (red) translucent ellipses represent positively (negatively) charged part. The blue arrow represents the direction of charge polarization which is defined as from negative charge to positive charge.

The same with AzoTMA, in both *trans*- and *cis*-tail, part B is negatively charged, both parts A and C are positively charged, and the two charge polarization directions change from opposite (*trans*) to a "V"-shape (*cis*). Furthermore, the charges in three parts of the *trans* tail molecule are 0.25 $h^+$, 0.51 $e^-$ and 0.26 $h^+$ respectively (Fig. S3a), which are almost the same with that of *trans*-AzoTMA (the charges are 0.25 $h^+$, 0.51 $e^-$ and 1.26 $h^+$ respectively, Fig. 2d) except that part C of *trans*-AzoTMA has one more positive charge which comes from the trimethylammonium group. Similarly, the charges of the *cis* tail (0.39 $h^+$, 0.80 $e^-$ and 0.41 $h^+$, Fig. S3b) are also the same with *cis*-AzoTMA (0.39 $h^+$, 0.80 $e^-$ and 1.41 $h^+$, Fig. 2e) except one more positive charge in part C. Therefore, after adding the trimethylammonium group to the tail molecule, only the charge in part C is changed, the charges in part A and B remain the same. So the effect of the head group is localized.

**S3. Hydroxylated α-quartz(001) surface**

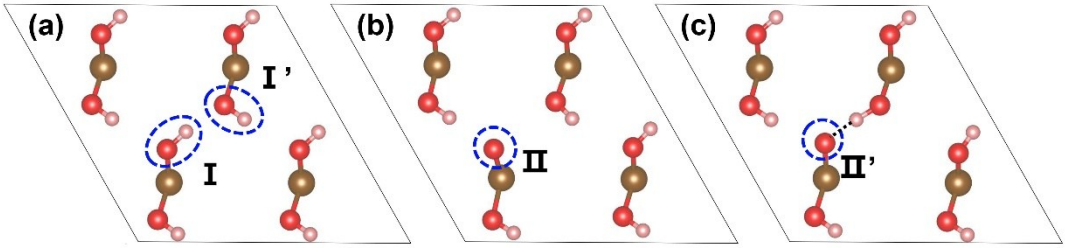


**Fig. S4.** Top view of the truncated fully hydroxylated α-quartz(001) surface (a) and two dehydrogenation surfaces (b) (c) in a 2×2 supercell.

There are two kinds of hydroxyl (I and I') on the fully hydroxylated α-quartz(001) surface as shown in Fig. S4a. Hydrion of hydroxyl on the surface is likely to be taken away by the hydroxide ion in aqueous solution. A dehydrogenation surface with an exposed oxygen atom (II) can be obtained when a hydroxyl in I site lost its hydrion (Fig. S4b). When a hydroxyl in I' site lost the hydrion, it will pull the neighboring hydrion and results in another dehydrogenation surface with an exposed oxygen atom (II', Fig. S4c).

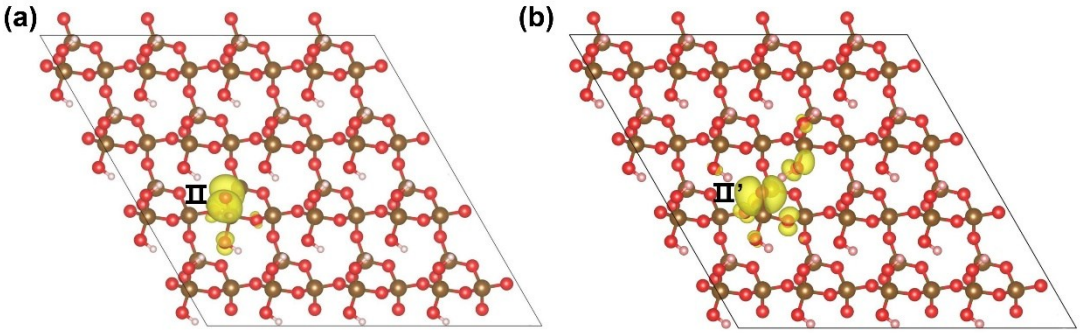


**Fig. S5.** The band decomposed charge density distribution at the valence band maximum (VBM) of surface II (c) and II' (d). The yellow isosurfaces represent electron distributions.

Charge density distributions at valence band maximum (VBM) of the two dehydrogenation surfaces show that the electron at VBM is mainly localized on the exposed oxygen atom (II/II' site in Fig. S5) and makes it negatively charged.

## S4. Adsorptions of AzoTMA on α-quartz(001) surface

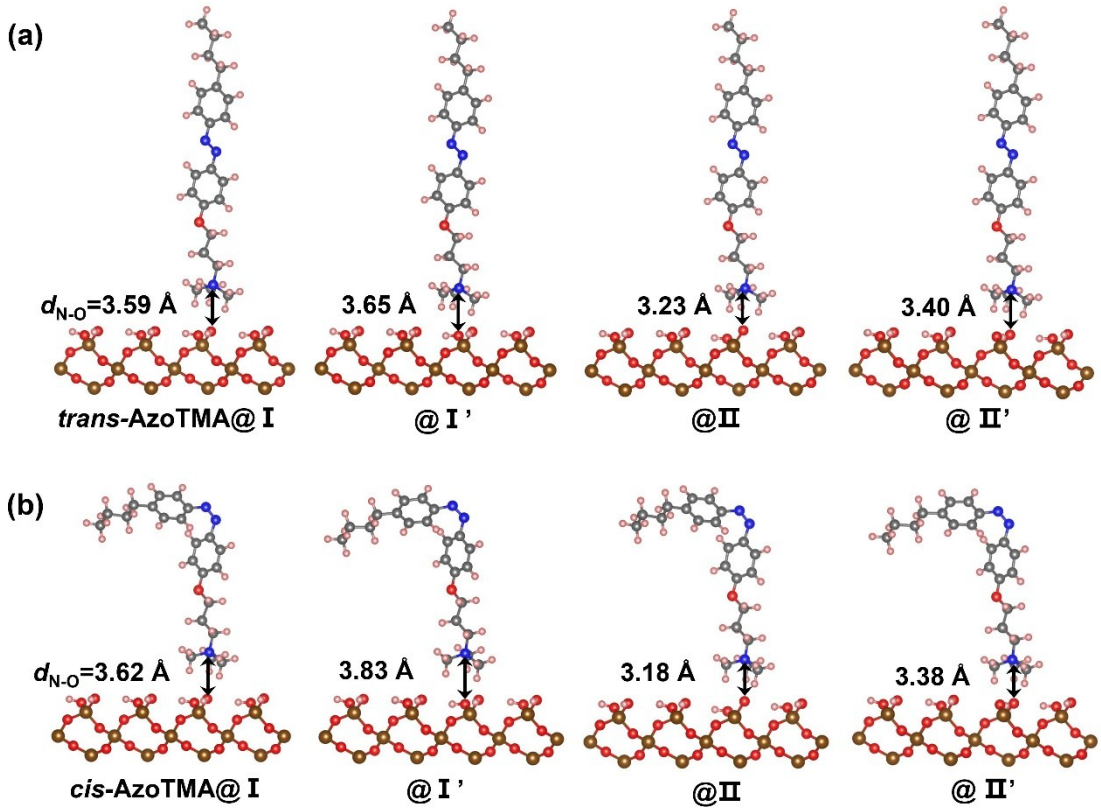


**Fig. S6.** (a) The optimized configurations of *trans*-AzoTMA adsorbed onto the I, I', II and II' site, respectively. (b) The optimized configurations of *cis*-AzoTMA adsorbed onto the I, I', II and II' site, respectively. $d_{N-O}$ is the distance between the nitrogen atom in head group of AzoTMA and the oxygen atom of adsorption site.

Table S4. Adsorption energies ($E_{ads}$) and charges donated from α-quartz(001) surface to AzoTMA obtained by Bander charge analysis

| **Adsorption site** | **$E_{ads}$ (eV)** | | **Charge (e$^-$)** | |
|---|---|---|---|---|
| | ***trans*** | ***cis*** | ***trans*** | ***cis*** |
| **I** | 1.35 | 1.30 | 0.031 | 0.027 |
| **I'** | 1.31 | 1.30 | 0.028 | 0.033 |
| **II** | 2.75 | 2.72 | 0.098 | 0.101 |
| **II'** | 2.44 | 2.44 | 0.083 | 0.080 |

The calculated adsorption energies ($E_{ads}$) of AzoTMA molecule adsorbed onto I and I' site which are both hydroxyls are about ~1.3 eV (Table S4), with small charge

transfers from the surface to AzoTMA (~0.03 $e^-$ in Table S4). However, when AzoTMA molecule adsorbed on the exposed oxygen atom (II or II' site), the adsorption energies are much larger than that on hydroxyl (increases are more than 1.0 eV, Table S4) due to the stronger electrostatic interaction (charge transfers are more than 0.08 $e^-$, Table S4). Consequently, AzoTMA molecules prefer to adsorb onto exposed oxygen atoms than hydroxyls on hydroxylated α-quartz(001) surface. Meanwhile, irrespective of which site is adsorbed on, the *trans*- and *cis*-AzoTMA exhibit very similar adsorption performance (differences of $E_{ads}$ are all less than 0.06 eV, Table S4) which means their interactions with silica surface are almost equivalent.

**S5. Experimental methods and results**

1) *Minerals and reagents*

Pure quartz mineral was provided by SKLE. These minerals were over 90% in purity based on mineralogical analysis and X-ray diffraction data. The photo-responsive surfactant, AzoTMA (4-butyl-(4'-(3-trimethylammoniumpropoxy)phenyl)azobenzene), was synthesized according to the procedures in reference 16. Its structure was shown in Fig. 1c. The purity of the surfactant was checked by $^{1}H$ NMR (Fig. 2c), using a Varianinova-400MHz NMR spectrometer.

UV light irradiation was done by a Prizmatix device equipped with photodiodes ( YL-512, Landun Photoelectricity, Guangdong, 365nm). Its maximal power was 10W (UV light) and the intensity of the light was 700 mW/cm$^2$. The surfactant solution was exposed for 30 min under UV light before use.

2) *Adsorption isotherms*

A mineral sample (1 g, -74+38 μm fractions) in 50 ml surfactant solution was added into a conical flask and shaken until the equilibrium was reached (24h). Then the sample was centrifuged for 20 min at 12000r/min. The surfactant concentration was immediately analyzed by total organic carbon analyzer (TOC-LCPH, Shimadzu Corporation). The results are the average of three independent measurements (measurement error<1%). Surface adsorption is calculated by the equation as follows:

$$\Gamma = (C_0\text{-}C)\ V/10^3 m$$

where $\Gamma$ is the surface adsorption (unit: mol/g); $C_0$ and C are the initial and residual

concentration of surfactant in suspension (unit: mol/l); V is the volume of the solution, (unit: ml); m is the amount of the quartz mineral sample (unit: g).

3) *Zeta potential*

The Zeta potential measurements were performed with a Zetapotential analyzer (Brookhaven Zeta Plus). A 10 mg sample (-5 μm) was placed in a 100 ml beaker and 30 ml solution of 1×10-3 mol/L KNO3 was used as the background electrolyte. The environmental temperature was maintained at 25.0±0.5℃. The results presented in the study were the average of five repeated measurements with a typical variation of ±2 mV.

**S6. Experimental results**

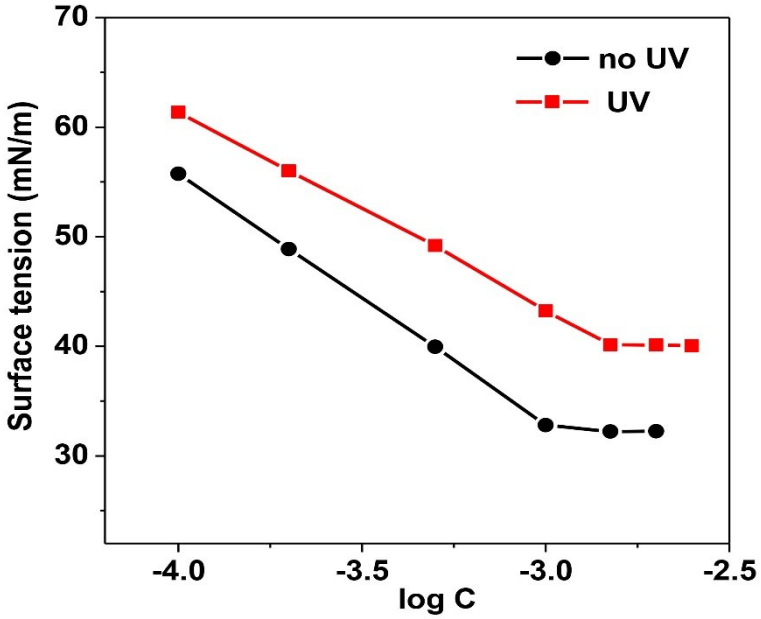


**Fig. S7.** Surface tension of AzoTMA aqueous solution versus the logarithm of concentration without UV (black line and plots) and under UV irradiation for 30 min (red line and plots).

According to Fig. S7, several physical-chemical parameters of AzoTMA could be generated as shown in Table S5. After UV irradiation, the critical micelle concentration, minimum surface tension and minimum cross sectional area all increase, and the saturated adsorption capacity decrease due to the *trans*→*cis* isomerization.

Table S5. The critical micelle concentration (cmc), minimum surface tension ($\gamma_{cmc}$), saturated adsorption capacity ($\Gamma_{max}$) and minimum cross sectional area ($A_{min}$) of AzoTMA

| Condition | cmc (mmol/L) | $\gamma_{cmc}$ (mN/m) | $\Gamma_{max}$ (μmol/m$^2$) | $A_{min}$ (nm$^2$) |
|---|---|---|---|---|
| **No UV** | 1.0 | 32.89 | 1.96 | 0.85 |
| **UV** | 1.5 | 39.93 | 1.48 | 1.12 |

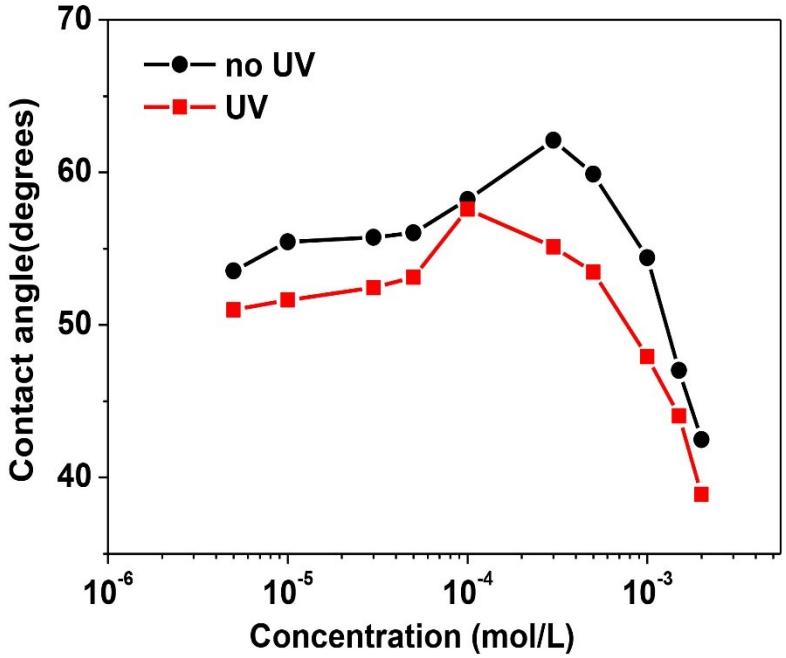


**Fig. S8.** Contact angle of AzoTMA aqueous solution on quartz versus concentration without UV (black line and plots) and under UV irradiation for 30 min (red line and plots).

Contact angle is usually used to measure the wettability of a solid surface. The contact angle of AzoTMA aqueous solution on quartz becomes smaller after UV irradiation at the same concentration (Fig. S8), indicating that the wettability of quartz surface is enhanced after UV irradiation.

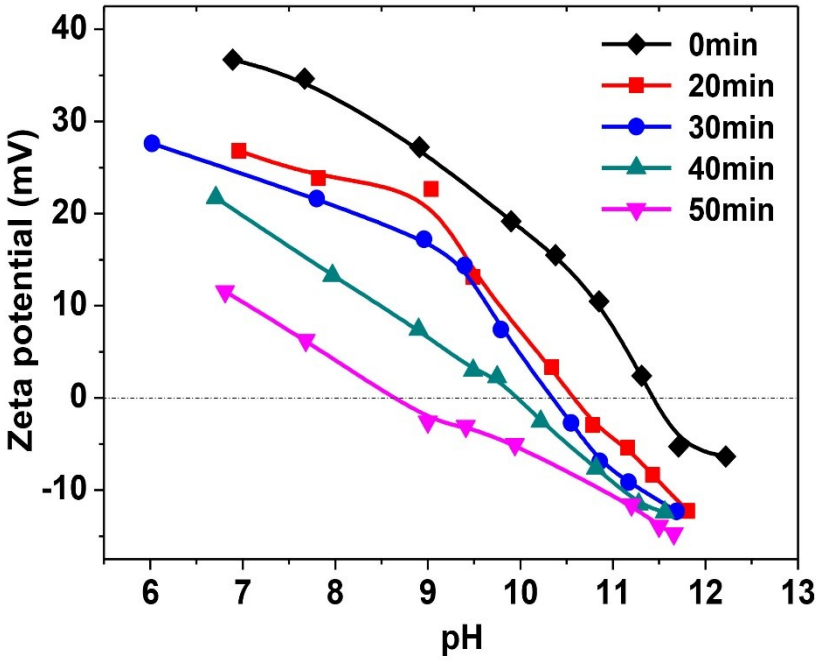


**Fig. S9.** Zeta potential of quartz versus pH under UV irradiation for different time.

As shown in Fig. S9, the zeta potential of quartz surface decreases with the increase of UV irradiation time due to the *trans*→*cis* isomerization which leads to the decrease in adsorption on the quartz surface. Meanwhile, the isoelectric point (the value of pH when the zeta potential is 0 mV) of quartz also decreases with the increase of UV irradiation time (Fig. S9).

## S7. Other computational results

We have also considered other reasons for the difference in adsorption behaviors of the two isomers of AzoTMA, two of which are charge transfer and proton transfer. We hypothesized that an electron transfer from azobenzene moiety to the head group would occur when the *trans*-AzoTMA molecule was excited by light, and then the positively charged head group would be neutralized with the transferred electron which resulted in desorption of AzoTMA from silica surface. However, the low excited states of *trans*-AzoTMA all show no charge transfer properties (Fig. S10a), and the lowest charge transfer state is the eighth excited state with a high excitation energy (Fig. S10b) which is difficult to be excited. Therefore, electron transfer is difficult to occur in *trans*-AzoTMA molecule.

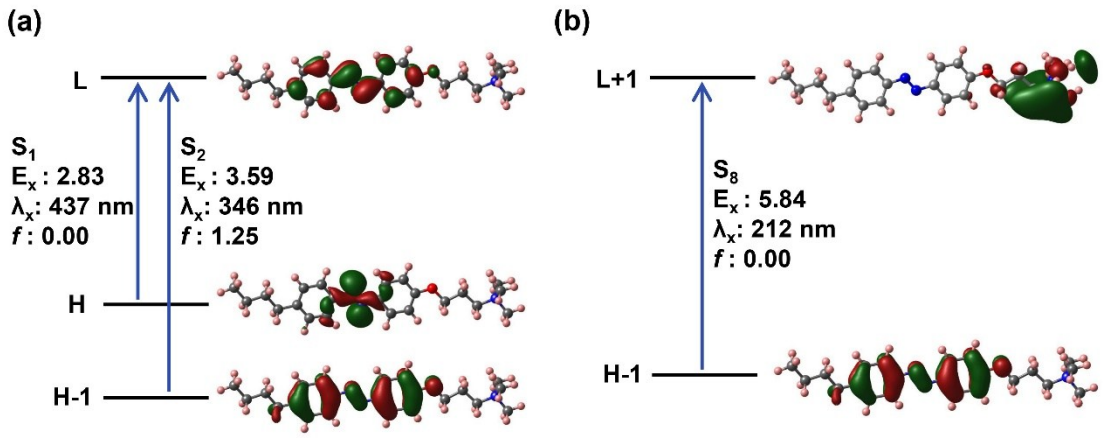


**Fig. S10.** (a) Electron transition of the excitation to the first excited state ($S_1$: HOMO→LUMO) and the second excited state ($S_2$: HOMO-1→LUMO) in *trans*-AzoTMA molecule. (b) Electron transition of the eighth excited state ($S_8$: H-1→L+1) which is a charge transfer state in *trans*-AzoTMA molecule.

Another hypothesis is the photo-induced proton transfer from water molecule to the oxygen atom of *trans*-AzoTMA and the remaining hydroxide of water will be attracted by the positively charged head group, which weakens the interaction between head group and silica surface and then lead to desorption of AzoTMA. Although the water molecule can be attached to the oxygen atom of *trans*-AzoTMA ($E_{ads}$ = 1.54 eV, Fig. S11a), it has little effect on the low excited states of *trans*-AzoTMA (Fig. S12), which means that the excited states do not involve the structural changes of water molecule. Moreover, the adsorption energy of a hydroxide to the head group of *trans*-AzoTMA is only 0.21 eV with a large adsorption distance (3.2 Å), indicating a very weak interaction between the hydroxide and the head group. More importantly, according to the above hypothesis, AzoTMA molecules will be desorbed from the silica surface if the hydroxide concentration increases, but the adsorption of AzoTMA grows when the pH increases (Fig. 4). So this hypothesis can also be ruled out.

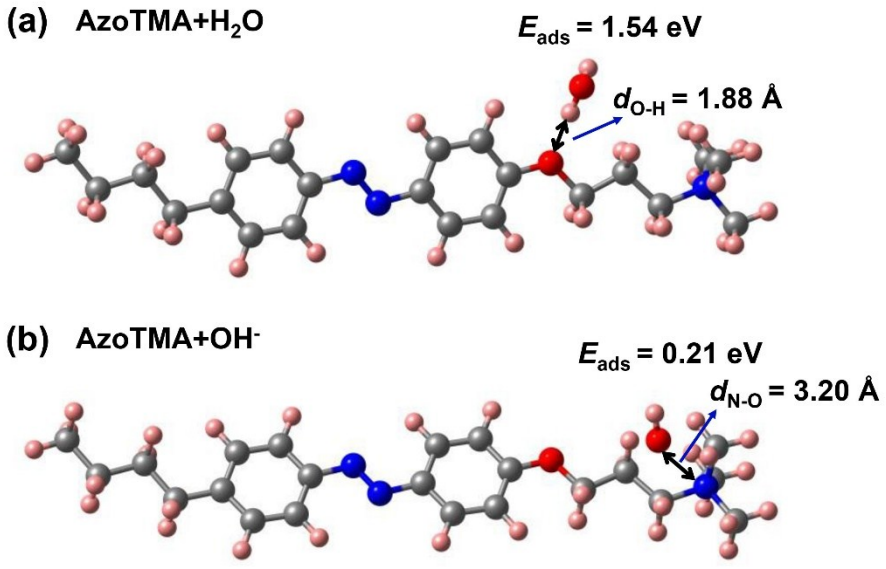


**Fig. S11.** (a) The optimized configurations of *trans*-AzoTMA adsorbed by a water molecule onto the oxygen atom together with the adsorption energy ($E_{ads}$) and distance

($d_{O\text{-}H}$). (b) The optimized configurations of *trans*-AzoTMA adsorbed by a hydroxide onto the head group together with the adsorption energy ($E_{ads}$) and distance ($d_{N\text{-}O}$)

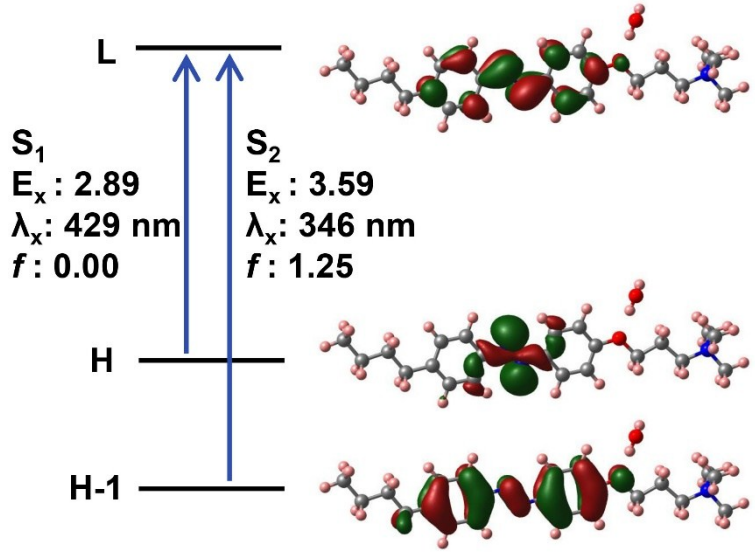


**Fig. S12.** Electron transition of the excitation to the first excited state ($S_1$: HOMO→LUMO) and the second excited state ($S_2$: HOMO-1→LUMO) in the complex system of *trans*-AzoTMA adsorbed by a water molecule.

**Reference**


1. Yanai, T.; Tew, D.P.; Handy, N. C. A new Hybrid Exchange-Correlation Functional using the Coulomb-Attenuating Method (CAM-B3LYP). *Chem. Phys. Lett.* **2004,** 393, 51-57.

2. F risch, M. J.; Trucks, G. W.; Schlegel, H. B.; Scuseria, G. E.; Robb, M. A.; Cheeseman, J. R.; Scalmani, G.; Barone, V.; Mennucci, B.; Petersson, G. A.; et al. *Gaussian 09*, Gaussian, Inc.: Wallingford, CT, USA, 2009.

3. Mennucci, B.; Tomasi, J.; Cammi, R.; Cheeseman, J. R.; Frisch, M. J.; Devlin, F. J.; Gabriel, S.; Stephens, P. J. Polarizable Continuum Model (PCM) Calculations of Solvent Effects on Optical Rotations of Chiral Molecules. *J. Phys. Chem. A* **2002,** 106, 6102-6113.

4. Jacquemin, D., Le Bahers, T., Adamo, C., Ciofini, I. What is the "Best" Atomic Charge Model to Describe Through-Space Charge-Transfer Excitations? *Phys. Chem. Chem. Phys.* **2012,** 14(16), 5383-5388.

5. Vignale, G. Real-time Resolution of the Causality Paradox of Time-Dependent Density-Functional Theory. *Phys. Rev. A* **2008,** 77, 062511.

6. Ho, J.; Klamt, A.; Coote, M. L. Comment on the Correct Use of Continuum Solvent Models. *J. Phys. Chem. A* **2010,** 114, 13442–13444.

7. Barone, V.; Cossi, M.; Tomasi, J. A new Definition of Cavities for the Computation of Solvation Free Energies by the Polarizable Continuum Model. *J. Chem. Phys.* **1997,** 107, 3210-3221.

8. Martínez, L.; Andrade, R.; Birgin, E. G.; Martínez, J. M. Packmol: A Package for

Building Initial Configurations for Molecular Dynamics Simulations. *J. Comput. Chem.* **2009**, 30, 2157-2164.

9. Stewart, J. J. P. Optimization of Parameters for Semiempirical Methods V: Modification of NDDO Approximations and Application to 70 Elements. *J. Mol. Modeling* **2007**, 13, 1173-1213.
10. Rezac, J.; Hobza, P. Advanced corrections of hydrogen bonding and dispersion for semiempirical quantum mechanical methods. *J. Chem. Theo. Comput.* **2012**, 8, 141-151.
11. Stewart, J. J. P. *MOPAC2016*. Colorado Springs, CO: Stewart Computational Chemistry.
12. Grimme, S.; Antony, J.; Ehrlich, S.; Krieg, H. A Consistent and Accurate Ab Initio Parametrization of Density Functional Dispersion Correction (DFT-D) for the 94 Elements H-Pu. *J. Chem. Phys.* **2010,** 132, 154104.
13. Kresse, G.; Furthmuller. J. Efficiency of Ab-Initio Total Energy Calculations for Metals and Semiconductors using a Plane-Wave Basis Set. *J. Comput. Mater. Sci.* **1996,** 6, 15–50.
14. Perdew, J. P.; Burke, K.; Ernzerhof, M. Generalized Gradient Approximation Made Simple. *Phys. Rev. Lett.* **1997,** 78, 1396.
15. Grimme, S. Semiempirical GGA-type Density Functional Constructed with a Long-range Dispersion Correction. *J. Comp. Chem.* **2006,** 27, 1787.
16. Chevallier, E.; Monteux, C.; Lequeux, F.; Tribet, C. Photofoams: Remote Control of Foam Destabilization by Exposure to Light using an Azobenzene Surfactant.

*Langmuir* **2012**, 28 , 2308-2312.